




Population Pharmacokinetic/Pharmacodynamic Analysis of the Glucokinase Activator PB201 in Healthy Volunteers and Patients with Type 2 Diabetes Mellitus: Facilitating the Clinical Development of PB201 in China

Ling Song^{1,2,3} · Fangrui Cao¹ · Shu Niu¹ · Michael Xu⁴ · Ruifang Liang⁴ · Ke Ding⁴ · Zhigang Lin⁴ · Xueting Yao¹ · Dongyang Liu^{1,3,5} 

Accepted: 11 October 2023 / Published online: 20 November 2023
© The Author(s), under exclusive licence to Springer Nature Switzerland AG 2023

Abstract

PB201 is an orally active, partial glucokinase activator targeting both pancreatic and hepatic glucokinase. As the second glucokinase activator studied beyond phase I, PB201 has demonstrated promising glycemic effects as well as favorable pharmacokinetic (PK) and safety profiles in patients with type 2 diabetes mellitus (T2DM). This study aims to develop a population PK/pharmacodynamic (PD) model for PB201 using the pooled data from nine phase I/II clinical trials conducted in non-Chinese healthy volunteers and a T2DM population and to predict the PK/PD profile of PB201 in a Chinese T2DM population. We developed the PK/PD model using the non-linear mixed-effects modeling approach. All runs were performed using the first-order conditional estimation method with interaction. The pharmacokinetics of PB201 were well fitted by a one-compartment model with saturable absorption and linear elimination. The PD effects of PB201 on reducing the fasting plasma glucose and glycosylated hemoglobin levels in the T2DM population were described by indirect response models as stimulating the elimination of fasting plasma glucose, where the production of glycosylated hemoglobin was assumed to be stimulated by fasting plasma glucose. Covariate analyses revealed enhanced absorption of PB201 by food and decreased systemic clearance with ketoconazole co-administration, while no significant covariate was identified for the pharmacodynamics. The population PK model established for non-Chinese populations was shown to be applicable to the Chinese T2DM population as verified by the PK data from the Chinese phase I study. The final population PK/PD model predicted persistent and dose-dependent reductions in fasting plasma glucose and glycosylated hemoglobin levels in the Chinese T2DM population receiving 50/50 mg, 100/50 mg, and 100/100 mg PB201 twice daily for 24 weeks independent of co-administration of metformin. Overall, the proposed population PK/PD model quantitatively characterized the PK/PD properties of PB201 and the impact of covariates on its target populations, which allows the leveraging of extensive data in non-Chinese populations with the limited data in the Chinese T2DM population to successfully supported the waiver of the clinical phase II trial and facilitate the optimal dose regimen design of a pivotal phase III study of PB201 in China.

1 Introduction

Diabetes mellitus is a worldwide-impacting metabolic disease featuring elevated blood glucose. Long-standing diabetes, if not well managed, can cause chronic damage and functional disabilities to various tissues/organs in the body, especially the eyes, kidneys, heart, blood vessels, and nervous systems, seriously affecting patients' quality of lives.

Among all diabetes cases, type 2 diabetes mellitus (T2DM) accounts for more than 90% [1] with metformin (MET) remaining its first-line pharmacological therapy. In the case where the target glycosylated hemoglobin (HbA1c) levels cannot be effectively achieved by MET monotherapy, dual or triple therapies combining MET with other drugs employing differed mechanisms of action (e.g., insulin secretagogues, alpha-glucosidase inhibitors, dipeptidyl peptidase 4 inhibitors, thiazolidinediones, sodium-glucose cotransporter 2 inhibitors, insulin or glucagon-like peptide-1 receptor agonists) are often required to provide better and persistent glycemic control [2]. Despite such a wide variety of available

Ling Song and Fangrui Cao equally contributed to this study.

Extended author information available on the last page of the article

Key Points

This work applied a population pharmacokinetic/pharmacodynamic strategy in the drug development of glucokinase activator PB201.

This study developed and qualified a population pharmacokinetic/pharmacodynamic model for PB201 using the pooled data from nine phase I/II clinical trials conducted in a non-Chinese population to predict the pharmacokinetic/pharmacodynamic profile of PB201 in a Chinese type 2 diabetes mellitus population.

The model-informed strategy in this work allowed us to predict the 24-week glycosylated hemoglobin level in a Chinese type 2 diabetes mellitus population and successfully supported the waiver of a clinical phase II study in China.

Additionally, this population pharmacokinetic/pharmacodynamic analysis informed the optimal dose selection (100 mg twice daily) for the Chinese phase III pivotal trial without conducting any additional clinical trials.

treatment options, only less than one third of the T2DM population had achieved the desired glycemic effects according to a large-scale survey in China [3]. With the increasing prevalence of T2DM [4], there is an urgent need to develop new chemical entities with the novel mechanism of action to be used either as monotherapy or in combination with the existing antidiabetic therapies to pursue further improvements in the management of T2DM.

Glucokinase (GK) [also called hexokinase IV] has become an emerging and outstanding target for the development of new antidiabetic drugs for T2DM owing to its critical role in glucose metabolism and regulation [5, 6]. It is primarily distributed in pancreatic β cells and hepatocytes facilitating the conversion of glucose to glucose-6-phosphate. Serving as a glucose sensor, GK increases or decreases insulin release by pancreatic β cells and glucose consumption by hepatocytes in response to rising or falling glucose levels, thus maintaining the homeostasis of glucose [7].

Glucokinase activators (GKAs) are a novel family of anti-diabetic drugs that targets GK. By controlling the confirmation of GK, GKAs maintain the activity of GK and

accelerate the phosphorylation of glucose in both pancreatic β cells and hepatocytes, thus offering dual correcting effects to restore/improve glucose homeostasis, for example, eliciting glucose-stimulated insulin secretion from the pancreas, and promoting hepatic glucose uptake and glycogen synthesis [8]. A number of small-molecule GKAs has been developed with some currently undergoing clinical investigation, which offers alternative strategies for the treatment of T2DM [8–11]. However, the clinical development of GKAs into later stages has experienced challenges because of the commonly occurring adverse effects (AEs) including hypoglycemia, increased liver burden, and diminishing efficacy over time [12–15]. Thus far, only two of the clinically tested GKAs have been studied beyond phase II, i.e., dorzagliatin and PB201, both of which have showed good research potential owing to high activity and low toxicity. Dorzagliatin, an orally bioavailable, dual-acting, full GKA that acts simultaneously on the pancreas and liver, has completed the phase III trial where it was shown to be effective in lowering blood glucose and well tolerated in a T2DM population who experienced inadequate control with MET alone when used as an add-on to MET [16].

PB201 (previously PF-04937319), initially developed by Pfizer and has been renamed PB201 since purchased by Pegbio Co., Ltd. (Suzhou, China) in 2016, was the second GKA to enter the phase III trial, which is currently recruiting participants in China (NCT05102149). PB201 is also an orally active, dual-acting GKA but was rationally designed as a partial GKA to maintain glucose-lowering efficacy while reducing the incidence of common AEs caused by GKAs [17]. So far, there has been a total of ten clinical trials of PB201 completed worldwide, which include nine phase I/II studies conducted in countries outside China and one phase I study conducted in a Chinese T2DM population. Existing clinical evidence has demonstrated promising glycemic effects of PB201 as well as favorable pharmacokinetic (PK) and safety profiles in both Chinese and non-Chinese populations [18–20].

In this study, we aim to best utilize all the existing clinical PK and pharmacodynamic (PD) data of PB201 across different populations to develop a population PK/PD (PopPK/PD) model. We hope to quantitatively characterize the relationships between PB201 plasma concentrations and the levels of PD markers (including fasting plasma glucose [FPG] and glycosylated hemoglobin [HbA1c]). We also aim to assess the potential covariates explaining the inter-individual variabilities (IIVs) of PK/PD (e.g., ethnic factors, disease status, food effects, co-medications). This PopPK/PD analysis aimed to leverage the quantitative PK/PD relationships from a non-Chinese population to a Chinese population and to facilitate the optimal dose selection and rationale study design for the subsequent clinical investigation of PB201 in China.

2 Methods

2.1 Clinical Study Design

The PopPK/PD model was developed and evaluated using data from seven phase I (NCT01044537, NCT01272804, NCT01513928, NCT01468714, NCT02206607, NCT02292433, and NCT01933672) and two phase II (NCT01517373 and NCT01475461) clinical trials. The study populations comprised healthy volunteers and a T2DM population of both sexes (age ≥ 18 years, body mass index: 17.5–45.4 kg/m²). PB201 was administered orally either as tablets or capsules with doses that ranged from 3 to 640 mg. The external validation of the PopPK/PD model was performed using the data from the phase I study conducted in 16 Chinese patients with T2DM (NCT03973515). A detailed summary of the clinical studies included in this PopPK/PD analysis is provided in Table 1.

2.2 Data Management

Patients and healthy individuals receiving placebo were excluded from the PopPK modeling database. Patients receiving the positive control drugs (i.e., glimepiride, sitagliptin) were excluded from both the PopPK and PK/PD datasets. If the missing data rate for PK or PD data was less than 10%, including missing data or values below the lower limit of quantification, these data were excluded from the dataset [21]. In multiple-dose studies, the administration time of the first dose was set to 0 with those of the subsequent doses calculated based on the difference between their actual dosing time and that of the first dose. Missing administration time for a later dose was imputed according to its dosing interval from the theoretical administration time of the first dose. Missing values of a covariate were replaced by the corresponding median values based on subjects of the same sex from the same study and the missing rate was less than 10%. For the PD model, the subject and/or study that lacked the PD data (FPG and HbA1c) after PB201 administration was also excluded from the analysis because of missing information on the PD characteristics.

2.3 Population PK/PD Model Development

The PopPK/PD model was developed by non-linear mixed-effects modeling with NONMEM (version 7.4; ICON Development Solutions, Ellicott City, MD, USA). NONMEM was implemented with PIRANA (version 2.8.0), PsN (perl-speaks-NONMEM, version 4.7; Uppsala, Sweden). All runs were performed using the first-order conditional estimation

method with interaction. R (version 3.6.2; Foundation for Statistical Computing, Vienna, Austria; <http://www.rproject.org>) was used for data management, statistics, and plotting.

A sequential modeling approach was utilized, i.e., a PopPK model was first developed using PK data of PB201 from both healthy subjects and the T2DM population. The individual PK parameters obtained from the PopPK model were used to estimate the PB201 plasma concentration at each of the timepoints for the subsequent development of the PopPK/PD model. For the PopPK/PD model, the FPG and HbA1c data in the T2DM population were utilized for the model development. The plasma concentration of PB201 was linked to the dynamic changes of FPG and then the FPG was driven by the dynamic characteristics of HbA1c.

The development of the PopPK and PK/PD models each involved three stages. First, a base structural model without considering the covariate effects was developed, which included the estimation of IIV and the residual variability using simplistic error models. For the PopPK model, we tested the one-compartment and two-compartment models with a first-order or non-linear absorption process. For the PK/PD model, various placebo model structures and drug effect structures were tested in the model development process (as shown in Appendix 1 of the Electronic Supplementary Material [ESM]). Second, a full multi-covariate model was developed after the addition of all statistically significant covariates to the base model. In the last stage, the final model was developed by removing the covariate-parameter combinations that made no statistically significant contribution to the model improvement.

As shown in Fig. 1, the base PK model features a one-compartment model with non-linear absorption of PB201 from the oral depot to the central compartment characterized by Michaelis–Menten kinetics and linear clearance from the central compartment. The differential equations are:

$$\frac{dA_a}{dt} = -\frac{V_m \times A_a}{K_m + A_a} \quad A_a(0) = \text{Dose} \times H, \quad (1)$$

$$\frac{dC_p \times V_c}{dt} = \frac{V_m \times A_a}{K_m + A_a} - \text{CL} \times C_p \quad C_p(0) = 0, \quad (2)$$

$$H = 1 - \frac{I_{\max} \times \text{DOSE}}{\text{IC}_{50} + \text{DOSE}}, \quad (3)$$

where V_m and K_m are the maximum absorption rate and the PB201 dose achieving 50% of V_m , A_a is the drug amount in the absorption compartment, C_p and V_c are the plasma concentration and volume of the central compartment, CL is the systemic clearance, H is the relative bioavailability, I_{\max} and IC_{50} are the maximum reductions of H and the PB201 dose achieving half I_{\max} , and DOSE refers to the dose of PB201.

Table 1 Summary of the clinical trials included the PK/PD model analysis

| Study no. | Phase | Study description | Dose (mg) | Subjects | PK samples ^a | PD samples ^a | Co-medication |
|--|-------|---|--|------------------------------------|-------------------------|--|---------------|
| NCT01044537 (B1621001) | I | Single-dose study | 10, 30, 100, 300, 480, and 640 mg | 50 subjects with T2DM | 13 | Plasma glucose: 9 | Metformin |
| NCT01272804 (B1621003) | I | Multiple-dose study | 10, 30, 50, 100 300 mg once daily | 61 subjects with T2DM | 28 | Plasma glucose: 61 (days 1–16) | Metformin |
| NCT01513928 (B1621005) | I | Cross-over (three periods) single-dose | 50 mg CR1 ^b ; 50 mg CR2; 50 mg IR | 12 healthy subjects | 18 for each period | NA | No |
| NCT01468714 (B1621011) | I | Estimate the steady-state effect of ketoconazole on the single-dose pharmacokinetics | 20 mg single dose on D1 and D6; ketoconazole 200 mg BID | 10 healthy subjects | 20 | NA | Ketoconazole |
| NCT02206607 (B1621015) | I | Cross-over (four periods) study of four oral formulations | IR MST: 150 mg/100 mg; MR formulation 1: 250 mg; MR formulation 2: 300 mg; MR formulation 3: 330 mg | 39 subjects with T2DM | 18 of each period | Plasma glucose 19 of each period | Metformin |
| NCT02292433 (B1621018) | I | 3-period, crossover study to assess the safety, pharmacokinetics/pharmacodynamics of two dose levels | Randomization sequences of 50 mg/50 mg, 150 mg/100 mg and placebo for three periods, each regimen dosed for 7 days | 12 Japanese patients with T2DM | 26 of each period | Plasma glucose: 32 of each period | No |
| NCT01933672 (B1621019) | Ib | 3-period, cross-over, active-controlled, multiple-dose study | Randomization sequences 300 mg QD; 150 mg/100 mg and sitagliptin 100 mg QD for three periods, each regimen dosed for 14 days | 33 patients with T2DM | 11 of each period | Plasma glucose: 14 of each period | Metformin |
| NCT01517373 (B1621002) | II | Placebo-controlled and active (glimepiride)-controlled, 5-arm (placebo, 3 active doses of PB201, and glimepiride), parallel-group study | 5 arm of 10, 50, and 100 mg PB201 once daily; placebo controlled and active (glimepiride) controlled | 304 patients with T2DM; 60 per arm | 6 trough concentrations | Plasma glucose: 9; HbA1c: 7 | Metformin |
| NCT01475461 (B1621007) | II | Placebo-controlled and active-controlled, 6-arm (placebo, 4 active doses of PB201, and 1 dose of sitagliptin), parallel-group study | 6 arms of 3, 20, 50, and 100 mg once daily; placebo controlled and active (sitagliptin, 100 mg QD) controlled | 335 patients with T2DM | 5 trough concentrations | HbA1c: 6; plasma glucose: 8; OGTT on day, 4 plasma glucose collection of each OGTT | Metformin |
| NCT03973515 (PB-2011116 ^c) | I | 4-period, cross-over multiple-dose study | Randomization sequences of 50/50 mg, 100/50, and 100 mg/100 mg, placebo | 16 Chinese patients with T2DM | 8 of each period | Continuous glucose monitoring data | No |

BID twice daily, *HbA1c* glycosylated hemoglobin, *IR* immediate release, *MR* modified release, *MST* material sparing tablet, *OGTT* Oral Glucose Tolerance Test, *PD* pharmacodynamic, *PK* pharmacokinetic, *QD* once daily, *T2DM* type 2 diabetes mellitus

^aNumber of sample timepoints per patient/group

^bCR1: shorter duration (~6 hours) of control release, CR2: longer duration (~14 hours) of control release

^cClinical data of the Chinese T2DM population were used for the model validation

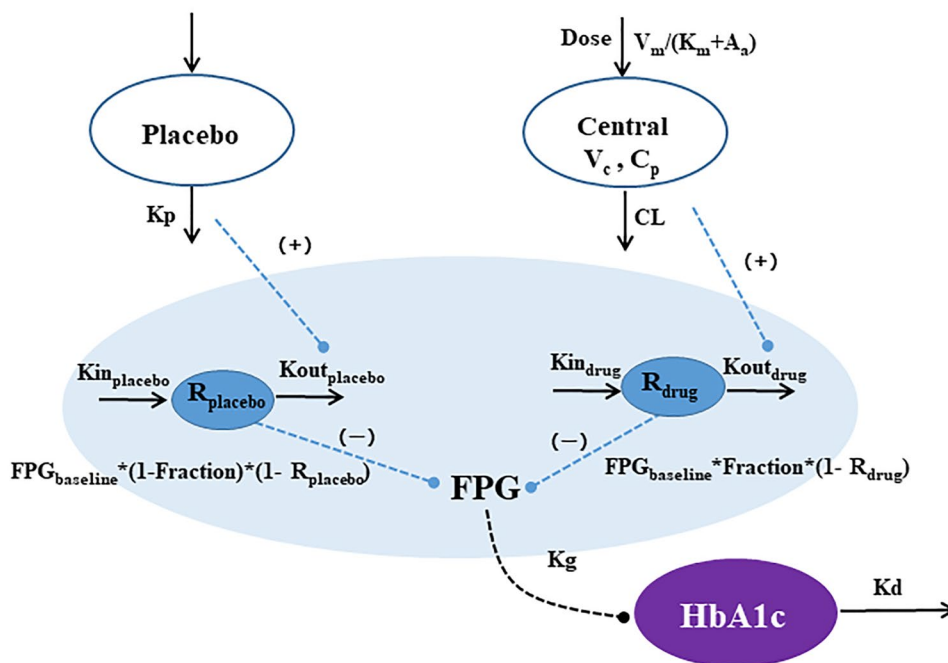


Fig. 1 Schematic of the pharmacokinetic/pharmacodynamic model structure. V_m and K_m are the maximum absorption rate and the PB201 dose achieving 50% of V_m , A_a is the drug amount in the absorption compartment, C_p and V_c are the plasma concentration and volume of the central compartment, and CL is the systemic clearance; we assumed that the percent changes in unphosphorylated glucose in pancreatic β cells and liver from baseline driven by the placebo

(R_{placebo}) and drug effects (R_{drug}). $K_{\text{in_placebo}}$ and $K_{\text{out_placebo}}$ are the synthesis and loss of R_{placebo} , $K_{\text{in_drug}}$ and $K_{\text{out_drug}}$ are the synthesis and loss of R_{drug} . The decreases of fasting plasma glucose (FPG) were proportional with $(1 - R_{\text{placebo}})$ and $(1 - R_{\text{drug}})$ with different scale factors, i.e., fraction for $(1 - R_{\text{drug}})$ and $(1 - \text{fraction})$ for $(1 - R_{\text{placebo}})$; K_g and K_d are the synthesis and loss of glycosylated hemoglobin (HbA1c)

The base PopPD model consists of multiple linked turnover models describing the dynamics of FPG and HbA1c. We assumed that the percent changes in unphosphorylated glucose in pancreatic β cells and liver from baseline were driven by the placebo (R_{placebo}) and drug effects (R_{drug}). R_{placebo} and R_{drug} were characterized by the indirect response models with placebo effects (placebo) and PB201 concentrations in the central compartment (C_p) as the driving forces stimulating the loss of responses ($K_{\text{out_placebo}}$ and $K_{\text{out_drug}}$). The decreases of FPG were proportional with $(1 - R_{\text{placebo}})$ and $(1 - R_{\text{drug}})$ with different scale factors, i.e., fraction for $(1 - R_{\text{drug}})$ and $(1 - \text{fraction})$ for $(1 - R_{\text{placebo}})$. The synthesis of HbA1c (K_g) was further stimulated by FPG [22]. The differential equations are as follows:

$$\frac{d\text{Placebo}}{dt} = -K_p \times \text{Placebo} \quad \text{Placebo}(0) = \text{Placebo}_{\text{baseline}}, \quad (4)$$

$$\frac{dR_{\text{placebo}}}{dt} = K_{\text{in_placebo}} - K_{\text{out_placebo}} \times R_{\text{placebo}} \times \left(1 + \frac{\text{Placebo}}{1000}\right), \quad (5)$$

$$\text{where } R_{\text{placebo}}(0) = 1; K_{\text{in_placebo}} = K_{\text{out_placebo}} \times R_{\text{placebo}}(0)$$

$$\frac{dR_{\text{drug}}}{dt} = K_{\text{in_drug}} - K_{\text{out_drug}} \times R_{\text{drug}} \times (1 + K \times C_p), \quad (6)$$

$$\text{where } R_{\text{drug}}(0) = 1; K_{\text{in_drug}} = K_{\text{out_drug}} \times R_{\text{drug}}(0)$$

$$\Delta\text{FPG}_{\text{drug}} = \text{FPG}_{\text{baseline}} \times \text{Fraction} \times (1 - R_{\text{drug}}), \quad (7)$$

$$\Delta\text{FPG}_{\text{placebo}} = \text{FPG}_{\text{baseline}} \times (1 - \text{Fraction}) \times (1 - R_{\text{placebo}}), \quad (8)$$

$$\text{FPG} = \text{FPG}_{\text{baseline}} - \Delta\text{FPG}_{\text{drug}} - \Delta\text{FPG}_{\text{placebo}}, \quad (9)$$

$$\frac{d\text{HbA1c}}{dt} = K_g \times \text{FPG} - K_d \times \text{HbA1c}, \quad (10)$$

$$\text{where } \text{HbA1c}(0) = \text{HbA1c}_{\text{baseline}}$$

$$K_g = \frac{K_d \times \text{HbA1c}_{\text{baseline}}}{\text{FPG}_{\text{baseline}}}, \quad (11)$$

where FPG is the fasting plasma glucose, placebo is the placebo effect, and K_p is the elimination rate constant of placebo. We assumed that the R_{placebo} and R_{drug} are the percentage changes from baseline in unphosphorylated glucose in pancreatic β cells and the liver for the placebo-treated and

drug-treated groups, $K_{in_placebo}$ and K_{in_drug} are the production rate constants of $R_{placebo}$ and R_{drug} , $K_{out_placebo}$ and K_{out_drug} are the elimination rate constants of $R_{placebo}$ and R_{drug} , K represents the inhibitory effects of PB201 concentrations on R_{drug} , $FPG_{baseline}$ and $HbA1c_{baseline}$ are the baseline values of FPG and HbA1c without any treatments, fraction is the percent reduction in FPG by R_{drug} , ΔFPG_{drug} and $\Delta FPG_{placebo}$ are the changes of FPG in subjects after receiving PB201 and placebo, and K_g and K_d are the synthesis and degradation rate constants of HbA1c.

In the base model, the IIV of PK or PD parameters were described by the exponential model, and a proportional error model was applied to describe the residual variability:

$$P_{ij} = \theta_i \times e^{\eta_{ij}}, \quad (12)$$

$$Y_{obs} = Y_{pred} \times (1 + \varepsilon), \quad (13)$$

where P_{ij} represents the i th parameter of the j th individual, θ_i is the typical value of population parameters, η_{ij} is the IIV of P_{ij} , η_{ij} follows a normal distribution with a mean of 0 and variance of ω^2 , Y_{obs} and Y_{pred} are the observed and predicted concentrations, and ε is the residual error following normal distribution with a mean of 0 and variance of σ^2 .

The potential correlations between individual PK or PD parameters of the final base structural model and various covariates including demographic covariates, disease status, relevant co-medications, and food effect were assessed to explore the sources of variability in the pharmacokinetics and pharmacodynamics of PB201. A complete list of covariates investigated was provided in Table S1 of ESM. An initial graphical analysis was performed to examine the extent and nature of the covariate–parameter relationships, for example, scatterplots for continuous covariates and boxplots for categorical covariates. A covariate was further included in a stepwise covariate screening procedure (i.e., forward selection followed by backward elimination) only when the covariate–parameter relationship showed a correlation coefficient > 0.3 . In the forward selection process, the selected covariates were added to the model individually and tested for statistical significance. The covariates were considered statistically significant and retained in the model when the change in the minimum value of the objective function was > 3.84 (based on $\chi^2_{\alpha=0.05, df=1}$). Subsequently, each covariate was removed from the full multi-covariate model using backward elimination and excluded from the final model if the change in the minimum value of the objective function was < 10.83 (based on $\chi^2_{\alpha=0.001, df=1}$). The IIV and residual error models were evaluated upon inclusion of all significant covariates in the final base model.

2.4 Model Qualification and Evaluation

The qualifications of both the base structural model and the final model were evaluated by standard goodness-of-fit plots. The predictive ability and accuracy of parameter estimates by the final model were evaluated by visual predictive check and bootstrap methods. The visual predictive check was performed with 1000 simulated datasets that were obtained based on the parameter values from the final model. The 5th, 50th, and 95th percentiles of the predicted concentration–time data were plotted and compared to those of the observed data to assess the agreement graphically. The bootstrap procedure involved fitting the final model to 500 datasets, each consisting of subjects resampled from the original dataset. The 95% confidence interval (CI) for the parameter obtained from each of the successful minimized models was calculated and compared to the original model-fitted parameter values.

2.5 Model Simulation to Support the Phase III Dose Regimen

To assess the applicability of the final PopPK model in Chinese populations, the concentration–time profiles of PB201 in 16 T2DM populations from the Chinese phase I study were simulated for 500 times and compared with the observed data. In the model simulations, PB201 was given with breakfast/lunch for 7 days with dosages of 50/50 mg, 50/100 mg, or 100/100 mg. A non-compartmental analysis (NCA) was performed using the linear up-log down approach in Phoenix WinNonlin version 8.1.0 (Certara, Princeton, NJ, USA). Descriptive statistics of the derived individual PK parameters (i.e., area under the concentration–time curve from time zero to 24 hours [AUC_{0-24}], maximum concentration [C_{max}], and half-life) based on the simulated data on days 1 and 7 were provided and compared to those obtained based on the observed data.

Then, the FPG and HbA1c profiles of 24 weeks were simulated under the potential phase III dose regimens (50 mg BID to 100 mg BID). The impacts of other selected covariates on the pharmacokinetics and pharmacodynamics of PB201 were also assessed using the final PopPK/PD model with the same dosing regimens of PB201 applied in PopPK model simulations. All model simulations in the Chinese T2DM population were performed based on the same demographic and laboratory covariate information as those in the original Chinese phase I study.

3 Results

3.1 Final PopPK/PD Model

For the PopPK model study, a total of 5061 PB201 concentrations from 555 subjects (22 healthy individuals and 533 individuals with T2DM) of all nine phase I/II studies were included in the final PopPK analysis. Subjects administered osmotic capsules (short and long durations of release) of study B1621005 and modified-release tablets of study B1621015 were excluded from the PopPK dataset as the exposure of these two special formulations were not bioequivalent for the immediate-release (IR) tablet. Twelve healthy subjects of study B1621005 and 39 individuals with T2DM with a single period of administered IR tablets were involved in the current PopPK model. No below the limit of quantification data were excluded from the current PPK model study. For the PopPD model, the final model was developed based on 3829 FPG and 2102 HbA1c concentrations from 596 patients with T2DM receiving placebo (146 patients) or PB201 (450 patients) of five phase I/II studies (B1621003, B1621018, B1621019, B1621002, B1621007). Studies B1621005 and B1621011 were excluded because no clinical PD data were collected in these two studies. Studies B1621001 and B1621015 were also excluded from the PopPD model study as these two studies lacked FPG data after multi-administration of PB201, which could not support the dynamic characteristics of FPG. No below the limit of quantification data were excluded from the current PopPD model study. In addition, six outlier FPG concentrations with conditional weighted residuals >6 were excluded from the current PopPD dataset. Detailed demographic and baseline information for the included subjects is listed in Table S1 of the ESM. As shown by the parameter estimates in Table 2, the pharmacokinetics of PB201 in both healthy subjects and the T2DM population were described by the one-compartment base model with non-linear absorption and linear elimination, with IIV being modeled on all PK parameters except for K_m : 34.4% for clearance, 11.6% for V_c , 51.6% for V_m , 16.7% for I_{max} , and 136% for IC_{50} . Initial graphical assessments revealed potential parameter covariate combinations (correlation coefficient > 0.3) for the PopPK model (Figs. S1–S4 of the ESM), and then stepwise covariate screening was performed. The ETA shrinkage for most PK parameters were within 30%. The shrinkage of IIV_ V_m was larger than 30%, which might interfere with the correlation assessment. In this study, we tested all available covariates (listed in Table S1 of the ESM) in the stepwise process. Finally, co-administration of ketoconazole and food effect were shown to significantly impact the pharmacokinetics

of PB201. The final covariate–parameter relationships were quantitatively described by the following equations:

$$CL = \theta_{CL} \times (1 + \theta_{CL-KTZ} \times KTZ), \quad (14)$$

$$V_m = \theta_{V_m} \times (1 + \theta_{V_m-FOOD} \times FOOD), \quad (15)$$

$$I_{max} = \theta_{I_{max}} \times (1 + \theta_{I_{max}-FOOD} \times FOOD), \quad (16)$$

$$IC_{50} = \theta_{IC_{50}} \times (1 + \theta_{IC_{50}-FOOD} \times FOOD), \quad (17)$$

where θ_{CL} is the typical clearance value of PB201 in the absence of ketoconazole co-administration; θ_{V_m} , $\theta_{I_{max}}$, and $\theta_{IC_{50}}$ are the typical value of V_m , I_{max} , and IC_{50} of PB201 when taken without food, KTZ and FOOD are the covariate indicators for co-administration of ketoconazole and food, the values of which equal to 1 or 0 indicate that PB201 is administered in the presence or absence of the covariates, and θ_{CL-KTZ} , θ_{V_m-FOOD} , $\theta_{I_{max}-FOOD}$, and $\theta_{IC_{50}-FOOD}$ represented the covariate effect on corresponding typical parameter values.

The parameter estimates obtained by the final PopPK model are listed in Table 2. After inclusion of the covariates into the base PopPK model, the IIV on clearance, V_c , V_m , I_{max} , and IC_{50} were decreased by 0.4%, 1.1%, 2.7%, 4.9%, and 11%, respectively, indicating that the covariate effects explained part of the IIV in these PK parameters. The systemic clearance of PB201 decreased by 10.5% when co-administered with ketoconazole. When PB201 is ingested with food, the maximum absorption rate (V_m) increased by 91.1%, the maximum reduction in bioavailability (I_{max}) decreased by 13.4%, and the dose achieving half I_{max} (IC_{50}) increased by 85.5%, suggesting that both the rate and extent of PB201 absorption were significantly increased by food.

With the individual PK parameters estimated from the final PopPK model, the plasma concentrations of PB201 of all timepoints were obtained and used in the subsequent PopPK/PD model development. The PK/PD relationships of PB201 were modeled using indirect response models where placebo effects and PB201 concentrations in the central compartment acted as the driving forces of stimulating FPG removal and the synthesis of HbA1c was stimulated by FPG (Fig. 1).

For the PopPD model, initial graphical evaluation of the covariate–parameter relationships (Figs. S3–S4 of the ESM) suggested that no covariates were significantly correlated with any PD parameters and thereby the base structural model was used as the final model. The parameters of the PK/PD model were estimated with low coefficient of variation values. The IIV estimated on PD parameters are 21.4% for $FPG_{baseline}$, 42.3% for fraction, and 11.6% for $HbA1c_{baseline}$, and all the ETA shrinkage was within 30% (Table 3).

Table 2 Population pharmacokinetic model parameters in the base model and final model (inclusion of covariates) of PB201

| Parameters (unit) | Definition | Base model | | Final model with covariates | | Bootstrap results |
|---|---|---------------|---------|-----------------------------|---------|--------------------|
| | | Estimates | RSE (%) | Estimates | RSE (%) | 95% CI |
| CL (L/h) | Clearance from central compartment | 16.6 | 4.6 | 15.4 | 5.3 | 13.5–17.8 |
| V_c (L) | Volume of distribution in central compartment | 182 | 4.9 | 166 | 5.6 | 147–192 |
| V_m (mg/h) | Maximum absorption rate constant | 107 | 11.2 | 66.9 | 11.9 | 42.4–114.2 |
| K_m (mg) | Dose corresponding to half of the maximum absorption rate | 96.6 | 17.0 | 96.0 | 18.1 | 48.9–201.4 |
| I_{max} | Maximum percentage reduction in bioavailability | 0.575 | 5.5 | 0.667 | 4.7 | 0.609–0.744 |
| IC ₅₀ (mg) | Dose corresponding to half the maximum reduction in bioavailability | 58.5 | 25.5 | 28.6 | 26.7 | 14.6–67.3 |
| CL-KET | Effect of ketoconazole co-administration on CL | NA | NA | – 0.105 | 16.1 | – 0.202 to – 0.021 |
| I_{max} -FOOD | Effect of food on I_{max} | NA | NA | – 0.134 | 22.6 | – 0.229 to – 0.065 |
| V_m -FOOD | Effect of food on V_m | NA | NA | 0.911 | 9.2 | 0.609–1.30 |
| IC ₅₀ -FOOD | Effect of food on IC ₅₀ | NA | NA | 0.855 | 47.1 | 0.201–1.58 |
| ω^2 CL [shrinkage] | IIV for CL | 34.4% [7.6%] | 3.5 | 34.0% [6.9%] | 3.5 | 30.9–36.8% |
| $\omega^2 V_c$ [shrinkage] | IIV for V_c | 11.6% [9.4%] | 30.6 | 10.5% [11.2%] | 40.5 | 2.3–17.1% |
| $\omega^2 V_m$ [shrinkage] | IIV for V_m | 51.6% [32.2%] | 6.9 | 48.9% [29.6%] | 7.4 | 47.1–67.9% |
| $\omega^2 K_m$ | IIV for K_m | 0 (fixed) | NA | 0 (fixed) | / | / |
| $\omega^2 I_{max}$ [shrinkage] | IIV for I_{max} | 16.7% [26.2%] | 23.3 | 11.8% [27.0%] | 27.8 | 1.7–15.8% |
| ω^2 IC ₅₀ [shrinkage] | IIV for IC ₅₀ | 136% [11.2%] | 12.6 | 125% [10.8%] | 11.8 | 77.0–166.6% |
| σ^2 [shrinkage] | Variance of proportional residual error in a pharmacokinetic model | 0.364 [6.3%] | 0.7 | 0.353 [6.0%] | 0.7 | 0.334–0.370 |

NA not available, CI confidence interval, CL clearance, IC₅₀, IIV inter-individual variability, I_{max} , K_m , NA, RSE relative standard error, V_c , V_m

The quality of the final PopPK/PD model was evaluated by the standard diagnostic plots (Figs. S5–S6 of the ESM), which revealed no significant systemic deviation or major bias. The visual predictive check plots (Figs. S7–S9 of the ESM) showed that the 5th, 50th, and 95th percentiles of the observed data generally fell within their corresponding 95% prediction intervals of the simulated data generated by 1000 model simulations, representing a good predictive performance of the PopPK/PD model. We also evaluated the current PopPK/PD model with the bootstrap approach. As shown in Tables 2 and 3, the parameter estimates obtained from the original models were included in the 95% bootstrap CI and were very close to

the bootstrap median values with sufficiently small relative standard errors (< 50%). These model evaluation results represented a good qualification of the final PopPK/PD model in describing the PK/PD characteristics of PB201 in non-Chinese healthy subjects and the T2DM population.

3.2 Simulation and Validation of the PK Profiles of PB201 in the Chinese Population

The applicability of the final PopPK model in Chinese populations was validated by the data from the Chinese phase I clinical study. The plasma concentration–time profiles of PB201 were simulated in 16 Chinese patients with T2MD

Table 3 Pharmacokinetic/pharmacodynamic model parameters of PB201

| Parameters (unit) | Definition | Estimates | RSE (%) | Bootstrap results, 95% CI |
|--|--|----------------|---------|---------------------------|
| FPG _{baseline} (mmol/L) | Baseline value of FPG | 9.00 | 1.2 | 8.83–9.17 |
| K _{p1} (L/h) | Placebo bio-phase rate constant of a short-period trial | 0.00954 | 29.7 | 0.01–0.02 |
| K _{p2} (L/h) | Placebo bio-phase rate constant of a long-period trial | 0.0593 | 15.8 | 0.035–0.082 |
| K _{out_{drug}} (L/h) | Elimination rate constant of variable drug-driven FPG change | 0.038 | 22.1 | 0.029–0.053 |
| K (mL/ng) | Drug effect of reducing drug-driven FPG change variable | 0.527 | 3.1 | 0.442–0.613 |
| K _{out_{placebo}} (L/h) | Elimination rate constant of placebo-driven FPG change variable; | 0.000510 | 12.2 | 0–0.001 |
| Fraction | Maximal fraction of drug-lowering effect of FPG | 0.915 | 2.7 | 0.862–0.958 |
| K _d (L/h) | Degradation rate constant of HbA1c | 0.000628 | 12.3 | 0.000486–0.000808 |
| HbA1c _{baseline} (%) | Baseline value of HbA1c | 7.80 | 0.8 | 7.71–7.89 |
| ω^2 FPG _{baseline} [shrinkage] | IIV for FPG _{baseline} | 21.4% [2.4%] | 3.8 | 11.8–33.0% |
| ω^2 Fraction [shrinkage] | IIV for fraction | 42.3% [18.2%] | 8.8 | 33.8–52.1% |
| ω^2 HbA1c _{baseline} [shrinkage] | IIV for HbA1c _{baseline} | 11.6% [14.6%] | 4.5 | 15.1–23.8% |
| σ^2 [shrinkage] | Variance of proportional residual error in a pharmacodynamic model | 0.0803 [11.5%] | 0.5 | 0.076–0.084 |

CI confidence interval, FPG fasting plasma glucose, HbA1c glycosylated hemoglobin, IIV interindividual variability

receiving 50/50-mg, 50/100-mg, or 100/100-mg oral doses of PB201 with food in the morning/noon for 7 consecutive days in the absence of ketoconazole. As shown in Fig. 2, the observed PB201 concentrations from all dosing groups fell within their corresponding 90% prediction interval of the simulated data and were evenly distributed around the 50th percentile of the simulated predictions, indicating a good agreement between the observations and model simulations. In addition, the PK parameters (AUC_{0-24} , C_{max} , and half-life) obtained by the NCA based on the observed time course data

after the first dose on day 1 and at steady state on day 7 were included in the 90% prediction interval of those obtained based on the simulated data (Table 4), further confirming the good predictive performance of the PopPK model on the pharmacokinetics of PB201 in Chinese populations. Additionally, current FPG and HbA1c models indicated no significant ethnic difference in the efficacy of PB201, which supported the long-term simulation of FPG and HbA1c in the Chinese T2DM population.

Fig. 2 Model simulated and observed PB201 concentration–time profiles in a Chinese type 2 diabetes mellitus population. Blue dots represent observations and black lines represent the 5th, 50th, and 95th prediction intervals. *hr* hour

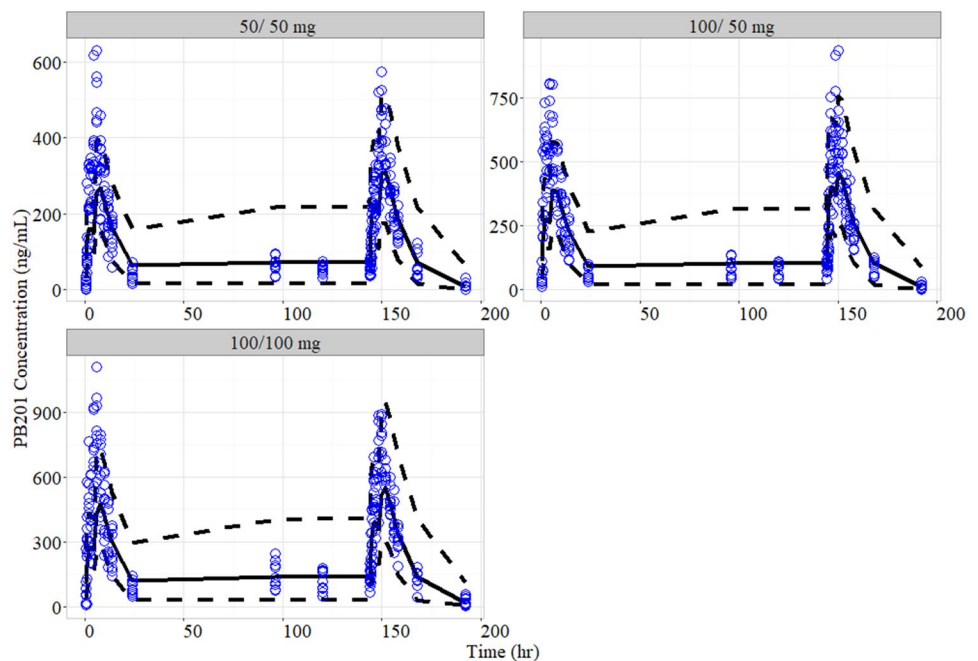


Table 4 Simulated pharmacokinetic parameters of multi-administration of PB201 in a Chinese type 2 diabetes mellitus population [median (90% prediction interval)]

| Parameters | Units | 50/50 mg | | 100/50 mg | | 100/100 mg | |
|--------------|----------|------------------|--------------------|--------------------|--------------------|--------------------|----------------------|
| | | Day 1 | Day 7 | Day 1 | Day 7 | Day 1 | Day 7 |
| AUC_{0-24} | hr*ng/mL | 4621 (1923–6307) | 5379 (2186–8809) | 6620 (2777–9541) | 7910 (3233–13,264) | 9281 (3391–11,663) | 11,122 (3897–16,230) |
| AUC_{inf} | hr*ng/mL | 4818 (2025–8975) | 5494 (2291–12,792) | 7016 (2903–13,442) | 8422 (3356–19,068) | 9623 (3561–16,667) | 11,641 (4064–23,566) |
| C_{max} | ng/mL | 279 (164–397) | 271 (178–513) | 555 (237–576) | 561 (264–754) | 504 (287–732) | 554 (315–932) |
| $t_{1/2}$ | hr | NA | 7.7 (4.3–12.9) | NA | 7.2 (4.2–13.0) | NA | 9.5 (4.3–12.8) |

AUC_{0-24} area under the concentration–time curve from time zero to 24 hours, AUC_{inf} area under the concentration–time curve from time zero to infinity, C_{max} maximum concentration, *hr* hour, $t_{1/2}$ half-life, *NA* not available

3.3 Simulation of Long-Term PK/PD of PB201 in a Chinese T2DM Population and the Waiver of the Clinical Phase II Trial

We simulated the steady-state exposure and long-term FPG and HbA1c profiles of PB201 in the Chinese T2DM population by considering the covariate effects. Food and co-administration of ketoconazole were found to increase the steady-state exposure of PB201 according to the final PopPK model-simulated PK profiles of PB201 in the Chinese T2DM population receiving 50 mg BID to 100 mg BID (Fig. 3 and Table 5). Steady-state AUC_{0-24} , C_{max} , and C_{min} of PB201 100 mg BID in patients computed by an NCA were increased by 12%, 8%, and 20% with the co-administration of ketoconazole, and were increased by 24%, 37%, and 8% as a result of the food effect. Although co-administration of MET was not found to be a significant covariate for the pharmacokinetics/pharmacodynamics of PB201 during the development of the PopPK/PD model using data from the non-Chinese populations, the baseline FPG of MET-treated patients are in general higher than those of the MET-naïve patients. Therefore, to better mimic the real situation of the phase II trials in the T2DM population where co-medication of MET is common, the quantitative relationship between $FPG_{baseline}$ and co-administration of MET obtained from the previous covariate selection process was included in the final PopPK/PD model to predict the PD characteristics of PB201 with or without the co-administration of MET in the Chinese T2DM population:

$$FPG_{baseline} = \theta_{FPG_{baseline}} \times (1 + \theta_{FPG_{baseline} - MET} \times MET), \quad (18)$$

where $\theta_{FPG_{baseline}}$ is the typical baseline FPG value of MET-naïve patients, *MET* is the covariate indicator, with the value of 1 or 0 indicating that PB201 is taken with or without MET, and $\theta_{FPG_{baseline} - MET}$ represents the proportional

change in FPG baseline with the co-administration of MET, which estimated as 0.684.

The model simulated FPG and HbA1c concentration–time profiles in the T2DM population after taking PB201 50/50 mg, 100/50 mg, or 100/100 mg with or without the co-administration of MET were displayed in Fig. 4 and Fig. S10 of the ESM. After correction by the placebo effects, the decreases in predicted mean concentrations from baseline in PB201 50/50-mg, 100/50-mg, and 100/100-mg treated groups are:

- 0.664 mmol/L, 0.894 mmol/L, 1.07 mmol/L for FPG, and 0.617%, 0.814%, and 0.964% for HbA1c when PB201 was given alone;
- 0.652 mmol/L, 0.952 mmol/L, 1.12 mmol/L for FPG, and 0.622%, 0.900%, and 0.980% for HbA1c when PB201 was co-administered with MET.

The model simulation results showed that persistent and dose-dependent decreases in FPG and HbA1c levels in the T2DM population were achieved by taking PB201 for 24 weeks with or without the co-administration of MET.

4 Discussion

PB201 was designed as a partial agonist for GK that exhibits a moderate binding affinity and fast dissociation [17, 23], aiming to maintain the desired glucose-lowering efficacy while mitigating the AEs caused by many other GKAs. As the second GKA that has entered phase II, the clinical development strategies and efficiencies for PB201 are of critical importance. The previous phase II clinical trials conducted in non-Chinese populations have demonstrated promising glycemic effects as well as good tolerance of PB201 [18, 19]. In the current study, we applied a popPK/PD approach to leverage extensive data in non-Chinese populations of

Table 5 Simulation of the covariate effect on the pharmacokinetic parameters of PB201 in Chinese patients with type 2 diabetes mellitus [median (range)]

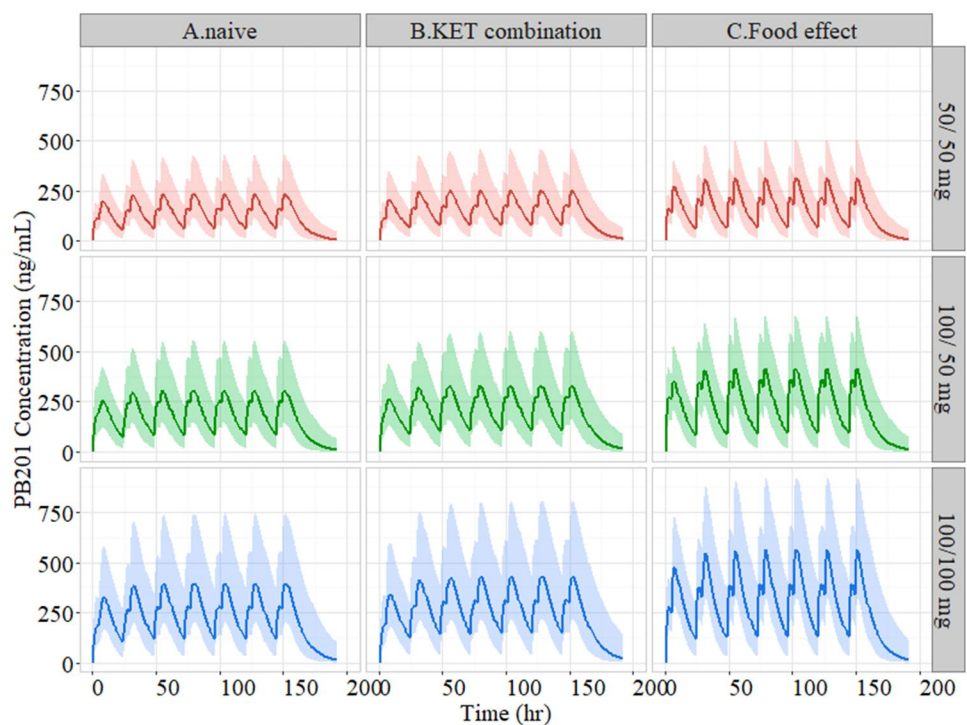
| Group | Parameters | Units | Naïve | KET combination | Ratio_KET ^a | FE | Ratio_FE ^b |
|------------|---------------------|----------|------------------|------------------|------------------------|------------------|-----------------------|
| 50/50 mg | AUC _{0–24} | hr*ng/mL | 3896 (3527–4430) | 4356 (3942–4951) | 1.12 | 4652 (4314–5227) | 1.19 |
| | C _{max} | ng/mL | 246 (226–270) | 266 (244–291) | 1.08 | 324 (307–347) | 1.32 |
| | C _{min} | ng/mL | 76 (65–98) | 92 (79–118) | 1.21 | 82 (69–104) | 1.07 |
| | T _{max} | hr | 8 | 8 | NA | 7 | NA |
| 100/50 mg | AUC _{0–24} | hr*ng/mL | 5308 (4534–5923) | 5923 (5067–6613) | 1.12 | 6627 (5746–7233) | 1.25 |
| | C _{max} | ng/mL | 326 (281–345) | 352 (304–374) | 1.08 | 431 (383–453) | 1.33 |
| | C _{min} | ng/mL | 103 (85–131) | 126 (103–156) | 1.21 | 116 (94–141) | 1.12 |
| | T _{max} | hr | 8 | 8 | | 7 | |
| 100/100 mg | AUC _{0–24} | hr*ng/mL | 7117 (6060–7660) | 7954 (6773–8560) | 1.12 | 8836 (7733–9470) | 1.24 |
| | C _{max} | ng/mL | 426 (379–464) | 461 (410–502) | 1.08 | 583 (532–630) | 1.37 |
| | C _{min} | ng/mL | 154 (116–167) | 184 (142–200) | 1.20 | 167 (131–182) | 1.08 |
| | T _{max} | hr | 8 | 8 | | 7 | |

NA not available, AUC_{0–24} area under the concentration–time curve from time zero to 24 hours, C_{max} maximum concentration, C_{min} minimum concentration, FE food effect, hr hour, KET ketoconazole, T_{max} time to C_{max}

^aRatio_KET is Exposure_{KET}/Exposure_{Naive}

^bRatio_FE is Exposure_{Food Effect}/Exposure_{Naive}

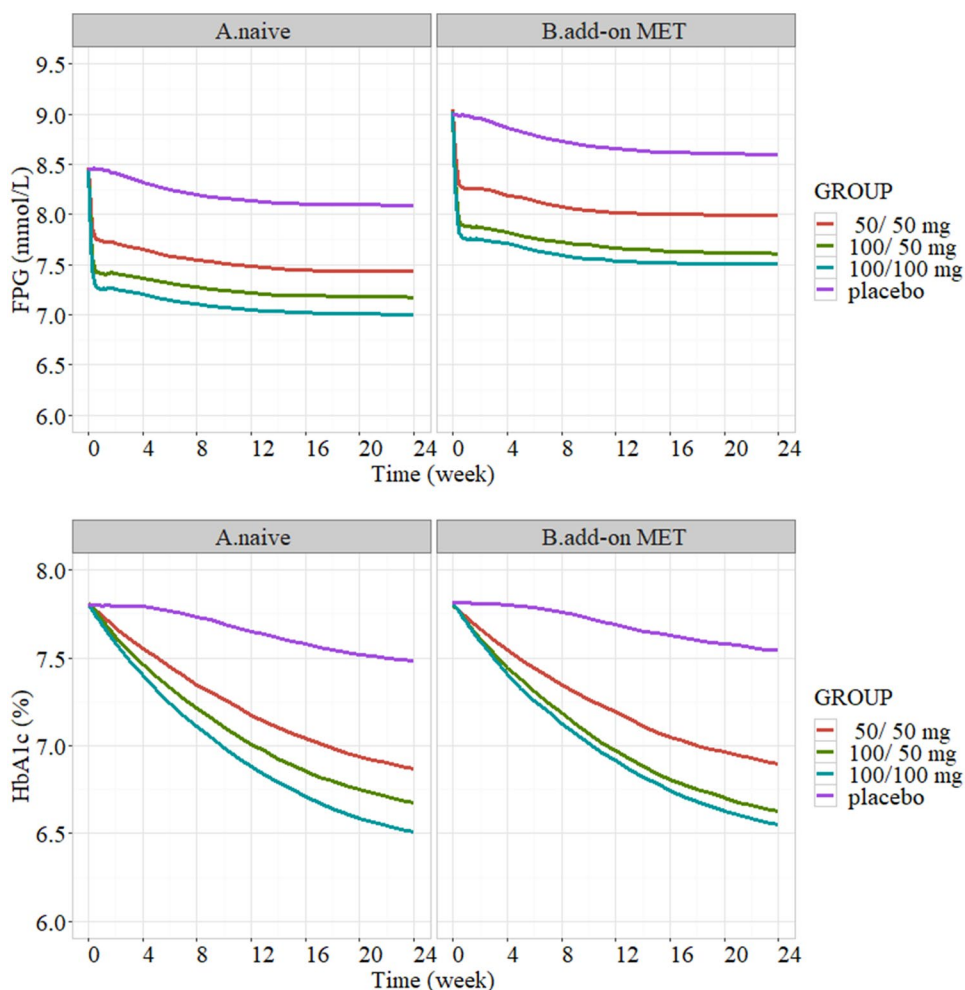
Fig. 3 Covariate effect of a ketoconazole (KET) combination and food effect on the pharmacokinetics of PB201 in a Chinese type 2 diabetes mellitus population. The line and ribbon represent the median and 90% prediction interval of predicted pharmacokinetics. hr hour



nine phase I/II studies of PB201 to successfully support the waiver of a clinical phase II trial and facilitate the optimal dose regimen design of a pivotal phase III study of PB201 in China.

In this study, we utilized PopPK/PD modeling and a simulation approach to support the optimal dose selection of 100 mg BID in a phase III study in a Chinese T2DM population without requiring additional clinical trials to be conducted. The dose of 100 mg QD studied in the non-Chinese phase Ib/

Fig. 4 Model-simulated fasting plasma glucose (FPG) and glycosylated hemoglobin (HbA1c) profiles in a Chinese type 2 diabetes mellitus population after administration of PB201 for 24 weeks. *MET* metformin



II studies exhibited comparable glucose-lowering efficacy to that offered by sitagliptin (NCT01475461), while it was not as effective as glimepiride (NCT01517373). Therefore, it is necessary to further evaluate the risk-to-benefit profiles at doses higher than 100 mg QD. The PK/PD of multiple doses of PB201 50/50 mg, 100/50 mg, and 100/100 mg BID have been assessed in the phase I study (NCT03973515) conducted in 16 drug-naïve Chinese T2DM populations [20]. This study showed that PB201 was well tolerated with low risks of hypoglycemia and other GKA-related side effects at doses up to 100 mg BID for 7 days [20]. In addition, dose dependent glucose-lowering effects were observed after the administration of placebo, PB201 50/50 mg, 100/50 mg, and 100/100 mg BID for 7 days. The least-square mean change in FPG from baseline was 0.31, -0.74 , -1.23 , and -1.47 mmol/L, respectively; the least-square mean change in 2-hour post-prandial plasma glucose from baseline was 0.83, -0.87 , -1.59 , and -1.88 mmol/L, respectively [20].

The results of the Chinese phase I study suggest that the 100-mg BID dose provides potentially better glycemic control than phase Ib and phase II doses tested (100 mg QD) in

non-Chinese populations [18, 19]. We developed the popPK/PD model by pooling the data of nine non-Chinese clinical trials of PB201 to simulate the long-term FPG and HbA1c profiles in a Chinese T2DM population. The model simulated results showed that the HbA1c decreased 0.769% and 0.974% after 12-week and 24-week administration of PB201 100 mg BID. The simulated glucose-lowering efficacy was comparable to that of glimepiride (NCT01517373) and better than that of sitagliptin (NCT01475461).

Additionally, in a total of ten completed clinical trials, PB201 was well tolerated in both healthy subjects and the T2DM population after multiple administrations [20]. No serious drug-related AEs were reported. For the AEs, 90.5% of them were mild in severity (Common Terminology Criteria for Adverse Events [CTCAE] Grade 1). We further analyzed the dose-dependent AEs (hypoglycemia and headache) at doses higher than 100 mg BID. The dose groups higher than 100 mg BID included five phase I studies in non-Chinese populations (300-mg, 480-mg, and 640-mg QD groups of B1621001; a 300-mg QD group of B1621003; 250-mg QD, 150/100-mg BID, and 300-mg QD groups of

B1621015; a 150/100-mg BID group of B1621018; 300-mg QD and 150/100-mg BID groups of B1621019) and one phase I study in a Chinese T2DM population (a 100/100 BID dose group in PB201116). There are 123 subjects with 267 AEs in these dose groups. Among them, the incidence of hypoglycemia and headache was 1.498% and 4.494%, respectively (unpublished data, Report No. PB-201-PM-01/CSR).

Finally, the model-simulated long-term FPG-HbA1c results after multiple administrations of PB201 were submitted to the Center for Drug Evaluation of China's National Medical Products Administration. Regulatory experts finally agreed on the waiver of a clinical phase II trial of PB201. The current model-simulated results supported the dose regimen of a pivotal phase III study with the dose of PB201 100 mg BID in China.

In the current popPK/PD modeling work, we aimed to accurately simulate the long-term PK/PD profiles in a Chinese T2DM population based on the short-term PK/PD data obtained from a Chinese phase I study. To accelerate the clinical development of PB201 in China, the main challenge of this modeling study was to bridge the PK/PD characteristics from non-Chinese to Chinese populations. We evaluate the ethnic differences in current popPK/PD modeling work. For the PK model, we first developed the popPK model of PB201 by pooling the data of nine phase I/II clinical studies conducted in a non-Chinese population to quantitatively characterize the PK/PD relationships of PB201 as well as the sources of variability. This model was then used to simulate the pharmacokinetics of PB201 based on the dose regimen and demographic characteristics of a Chinese phase I study (PB-201116). External validation was performed using the PK data of a phase I clinical study conducted in a Chinese T2DM population.

This PopPK model showed a favorable predictive performance in a Chinese T2DM population and further indicated no significant ethnic influences on PB201 pharmacokinetics. For the PD model, to support the leveraging of PD from the non-Chinese population to the Chinese population, we compared the predicted FPG and HbA1c in the Chinese population to the observed PD data in the non-Chinese population. We simulated the 12-week FPG and HbA1c profiles utilizing Chinese population characteristics based on study PB201116. The simulated dose regimen was based on two non-Chinese phase II clinical trials (B1621002 and B1621007) for efficacy dose levels of 50 mg and 100 mg. The simulated FPG and HbA1c data after the administration of PB201 for 12 weeks showed good agreements with clinically observed data (Fig. S11 of the ESM). The predicted FPG and HbA1c of the Chinese T2DM population were 8.14 mmol/L [5.52–12.2 mmol/L] and 7.28% [range 5.98–8.98 %] (represented as median [90% prediction interval]) after 100-mg QD administration of PB201 for 12 weeks, which

were consistent with the corresponding observed FPG and HbA1c data of 8.02 mmol/L [6.31–12.5 mmol/L] and 7.10% [6.31–9.30%] (represented as median [90% prediction interval]) in non-Chinese Asian patients. The simulated results initially supported the leveraging of the pharmacodynamics from the non-Chinese population to the Chinese population.

The pharmacokinetics of PB201 in both healthy individuals and T2DM population were best described by a one-compartment PopPK model with non-linear absorption. The wide dose range (10–640 mg) of PB201 used in the clinical studies allowed the characterization of the non-linearities in pharmacokinetics. The pre-clinical PK study in rats also supported the non-linear pharmacokinetics of PB201, in which the exposure increasing was less than dose proportional at the dose level of 50–1000 mg (unpublished data). PB201 was not a potential substrate of intestinal transporters. PB201 belonged to the Biopharmaceutics Classification System IV with moderate permeability ($16.7\text{--}27.5 \times 10^{-6}$ cm/s) and poor solubility. Hence, the saturated absorption might be attributed to the poor solubility of PB201 (unpublished data), which resulted in the dose-dependent reduction in bioavailability. In the current PPK model, we described the dose-saturated relative bioavailability as model parameter H. This parameter decreased with the dosage increasing. The H was around 50–60% at the dose level of 600 mg, which was consistent with the results obtained by an NCA (as shown in Table S2 of the ESM).

In addition, we also evaluated the effect of different formulations on the bioavailability in the current PopPK model. In this study, we only involved the subjects receiving the tablets or capsules. The osmotic capsules (short and long duration of controlled release [CR]) and the modified-release tablets were not involved in the PopPK model, as the exposure of these two special formulations were not bioequivalent to the IR tablet. For the CR capsules (study B1621005), the AUC_{0-24} of CR1 (shorter duration [~6 hours] of CR) and CR2: (longer duration (~14 hours) of CR) were 88.0% and 69.0% of that for the IR tablet, the C_{max} of CR1 and CR2 were 64.0% and 31.0% of IR. For the MR tablets (study B1621015), the AUC_{0-24} of MR1, MR2 and MR3 were 31.1%, 25.0%, and 31.7% of IR, the C_{max} of MR1, MR2, and MR3 were 25.2%, 26.4%, and 36.9% of IR. While, for the IR capsules and IR tablets, no significant difference in the pharmacokinetic was observed. We compared the basic PK parameters and PK profiles of the same dose group of IR capsules (study B1621001, total 23 subjects of 10-mg, 30-mg, 100-mg, and 30-mg dose group) and IR tablets (B1621003, total 36 subjects of 10-mg, 30-mg, 100-mg, and 300-mg dose group). The ratios for C_{max} , time to C_{max} and AUC_{0-24} were within 0.99–1.51-fold, 0.83–1.17-fold, and 0.96–1.36-fold (as shown in Table S3 of the ESM). Of course, the covariates analysis also demonstrated that IR

capsules or tablets did not affect the PK characteristics of PB201.

The time courses of FPG and HbA1c concentrations in the T2DM population after receiving placebo or PB201 were reasonably characterized by a PopPD model with multiple indirect response models where the removal of FPG was stimulated by both the placebo effects and the plasma concentration of PB201. For the placebo model structure, we have tested various classic placebo models during the model development process (including the simpler time-variant placebo effect model; the time-variant placebo effect model incorporating disease progression), the detailed model testing process was shown in Appendix 1 of the ESM. However, we could not use the above model structures to describe the current placebo effect, which might be owing to the complexity of the placebo data in the current study. The individual placebo FPG profiles had large IIV, even the FPG changed direction (increase, unchanged, or decrease) of different placebo groups was not consistent. All the above placebo model structures were difficult to fit the observed FPG data in the placebo group. Hence, we finally described the placebo effect with a fit-for-purpose model, which handled the placebo effect with a hypothetical bio-phase placebo compartment as previously reported [22]. In addition, for the drug effect model, we adopted FPG as the PD marker to drive the HbA1c with the following considerations: (1) FPG was the primary PD marker in clinical phase I/II trials of PB201, which provided rich data for model development; (2) pre-prandial glucose values had a stronger association with HbA1c than post-prandial glucose for type 1 and 2 diabetes, particularly for T2DM [24]; and (3) although the continuous glucose monitoring data also have the better association with HbA1c [24], the CGM data of PB-201 were limited (only collected in one phase I study, PB201116). Based on the above considerations, the hypothetical bio-phase placebo compartment and drug compartment were linked to two indirect response models (R_{placebo} and R_{drug}) to represent the percent changes in un-phosphorylated glucose in pancreatic β cells and the liver from baseline driven by the placebo and PB201. The PB201 concentration was added on the elimination of R_{drug} owing to the mechanism of GKA, i.e., accelerating the hypothetical phosphorylation of un-phosphorylated glucose. We tested the linear model and E_{max} model to describe the FPG effect, and the linear model described the model well (as shown in Appendix 1 of the ESM). For most of the hypoglycemic drugs (including the GKAs), the drug effect diminishes over time because of disease progression and placebo effects [25]. In this study, we used the indirect response model of R_{drug} to characterize the diminished effect of PB201 over time because of the disease progression. Then, the placebo effect and drug effect simultaneously described the FPG profiles [22]. Finally, another indirect response model structure was adopted to

describe the synthesis of HbA1c that was driven by FPG. We involved 3829 observed FPG data points and 2102 HbA1c data points from 596 patients with T2DM in our PD model. For two pivotal phase II studies, each individual subject had eight to nine FPG data points and six to seven HbA1c data points, all of these data were included in the current PD model. Hence, the FPG and HbA1c data were relatively rich for estimating the PD model parameters, which could be demonstrated by the small ETA shrinkage of all the PD parameters (less than 30%).

We accessed the correlation between the IIV of PK/PD model parameters and potential covariates based on the established ETA shrinkage values of model parameters being within a good acceptable range (within 30%) [26]. All the potential covariates listed in Table S1 of the ESM were included in the correlation analysis (Figs. S1–S4 of the ESM). We involved all the continuous covariates and categorical covariates in the stepwise analysis although the Exploratory data analysis showed that all correlation coefficients of continuous covariates were less than 0.3. The covariate screening revealed that food and co-administration of ketoconazole were statistically significant covariates on the PK parameters of PB201. When PB201 was given with food, its maximum percentage reduction in the bioavailability (I_{\max}) was decreased. The PB201 dose achieving 50% I_{\max} (IC_{50}) and the maximum absorption rate (V_m) was increased, suggesting that both the rate and extent of absorption of PB201 was increased by food. It was reported that PB201 is metabolized primarily mediated by CYP3A and CYP2C isoforms [27]. Thus, it is not surprising that the co-administration of ketoconazole, a potent CYP3A inhibitor, reduces the systemic clearance of PB201. However, the steady-state area under the concentration–time curve of PB201 was not significantly affected by food and co-administration of ketoconazole (within 80–125%) as shown in Fig. 3 and Table 5. Although the datasets used to develop the PopPK/PD model consisted of multiple ethnic groups including Caucasian, African American, and non-Chinese Asian individuals, ethnicity was not shown to be a significant covariate on either the pharmacokinetics or pharmacodynamics of PB201. The PK characteristics in the T2DM population and healthy subjects showed no significant difference. The forward step showed that the OFV decreased less than 3.84 when this categorical covariate (healthy subjects or patients with T2DM) was involved in the PK base model, which initially indicated that the T2DM disease state has no significant effect on PB201 pharmacokinetics. However, the sample size was small for healthy subjects in the current PopPK study and the influence of the disease state needs to be verified in future larger populations. For the PD model, no covariates were found to significantly impact the pharmacodynamics of PB201. Metformin is one of the first-line hypoglycemic drugs. The metformin added-on T2DM

population often features a higher FPG baseline and a longer disease progression than the naïve T2DM population, which is consistent with our data exploratory analysis results (as shown in Fig. S4 of the ESM). Hence, we involved the MET effect on FPG baseline in the current model to quantify the differences between add-on and naïve T2DM populations. Nevertheless, because of the data limitation (only phase I and phase II populations), the non-significant covariates informed by the current PK/PD model should not be completely ignored in the subsequent phase III clinical study. In future work, the model-informed covariate effects on the PK/PD characteristics of PB201 still need further evaluation by phase III clinical trials by combining other pharmacometric approaches, such as physiologically based pharmacokinetic model and exposure-response analyses.

5 Conclusions

The PopPK/PD model developed in this work allowed the quantitative characterization of the PK/PD relationships of PB201 as well as the identification of potential covariates explaining the IIVs. The PopPK/PD model was initially developed in non-Chinese populations, externally validated by the PK profiles of multiple administrations in a Chinese T2DM population. Then, the model was applied to simulate the time courses of FPG and HbA1c concentrations in a Chinese T2DM population. According to the PopPK/PD model-predicted long-term glucose-lowering efficacy of PB201 in a Chinese T2DM population as well as the exposure–safety relationship analysis, the dose of PB201 100 mg taken twice daily exhibited a favorable risk-benefit profile. This PopPK/PD analysis has played a significant role in bridging the existing clinical data of PB201 from multiple non-Chinese populations to inform the optimal dose selection for the Chinese phase III pivotal trial without the need for conducting any additional clinical trials.

Supplementary Information The online version contains supplementary material available at <https://doi.org/10.1007/s40262-023-01321-8>.

Declarations

Funding The study was supported by the National Natural Science Foundation of China (no. 82173895 and no. 82373954), The Bill & Melinda Gates Foundation (Grant/Award Number: INV-007625) and the Peking University Third Hospital Clinical Project (Grant/Award Number: BYSYFY2021006).

Conflicts of interest/competing interests Michael Xu, Ruifang Liang, Ke Ding, and Zhigang Lin are employees of PegBio Co., Ltd., (Suzhou, Jiangsu, China) the company that owns PB201. Ling Song, Fangrui Cao, and Dongyang Liu have no conflicts of interest that are directly relevant to the content of this article.

Ethics approval The data used in this study were collected in line with the principles of the Declaration of Helsinki. Approval was granted by institutional review boards and independent ethics committees for each study of which data were used in this work.

Consent to participate Not applicable.

Consent for publication Not applicable.

Availability of data and material All data generated or analyzed during this study are included in this published article (and its supplementary information files).

Code availability Not applicable.

Authors' contributions LS, FC, and DL designed the study. LS and FC conducted the modeling and simulation work. MX, RL, KD, and ZL provided the clinical raw data.


References

- American Diabetes Association Professional Practice Committee. 2. Classification and diagnosis of diabetes: standards of medical care in diabetes-2022. *Diabetes Care*. 2022;45(Suppl. 1):S17–38.
- American Diabetes Association Professional Practice Committee. 9. Pharmacologic approaches to glycemic treatment: standards of medical care in diabetes-2022. *Diabetes Care*. 2022;45(Suppl. 1):S125–43.
- Ji LN, Lu JM, Guo XH, Yang WY, Weng JP, Jia WP, et al. Glycemic control among patients in China with type 2 diabetes mellitus receiving oral drugs or injectables. *BMC Public Health*. 2013;21(13):602.
- Lin X, Xu Y, Pan X, Xu J, Ding Y, Sun X, et al. Global, regional, and national burden and trend of diabetes in 195 countries and territories: an analysis from 1990 to 2025. *Sci Rep*. 2020;10(1):14790.
- Matschinsky FM, Wilson DF. The central role of glucokinase in glucose homeostasis: a perspective 50 years after demonstrating the presence of the enzyme in islets of Langerhans. *Front Physiol*. 2019;10:148.
- Doliba NM, Qin W, Najafi H, Liu C, Buettger CW, Sotiris J, et al. Glucokinase activation repairs defective bioenergetics of islets of Langerhans isolated from type 2 diabetics. *Am J Physiol Endocrinol Metab*. 2012;302(1):E87–102.
- Matschinsky FM. Glucokinase, glucose homeostasis, and diabetes mellitus. *Curr Diab Rep*. 2005;5(3):171–6.
- Ren Y, Li L, Wan L, Huang Y, Cao S. Glucokinase as an emerging anti-diabetes target and recent progress in the development of its agonists. *J Enzyme Inhib Med Chem*. 2022;37(1):606–15.
- Spasov AA, Lobasenko VS, Kosolapov VA, Babkov DA, Kuznetsova VA, Maika OY, et al. Synthesis and pharmacological activity of 3-phenoxybenzoic acid derivatives. *Pharm Chem J*. 2020;54(3):229–35.
- Dzyurkevich MS, Babkov DA, Shtyrlin NV, Mayka OY, Iksanova AG, Vassiliev PM, et al. Pyridoxine dipharmacophore derivatives as potent glucokinase activators for the treatment of type 2 diabetes mellitus. *Sci Rep*. 2017;7(1):16072.
- Li W, Zhang X, Sun Y, Liu Z. Recent clinical advances of glucokinase activators in the treatment of diabetes mellitus type 2. *Pharmazie*. 2020;75(6):230–5.
- Toulis KA, Nirantharakumar K, Pourzitaki C, Barnett AH, Taharani AA. Glucokinase activators for type 2 diabetes: challenges and future developments. *Drugs*. 2020;80(5):467–75.

13. Zhi J, Zhai S. Effects of piragliatin, a glucokinase activator, on fasting and postprandial plasma glucose in patients with type 2 diabetes mellitus. *J Clin Pharmacol*. 2016;56(2):231–8.
14. Kiyosue A, Hayashi N, Komori H, Leonsson-Zachrisson M, Johnsson E. Dose-ranging study with the glucokinase activator AZD1656 as monotherapy in Japanese patients with type 2 diabetes mellitus. *Diabetes Obes Metab*. 2013;15(10):923–30.
15. Meininger GE, Scott R, Alba M, Shentu Y, Luo E, Amin H, et al. Effects of MK-0941, a novel glucokinase activator, on glycemic control in insulin-treated patients with type 2 diabetes. *Diabetes Care*. 2011;34(12):2560–6.
16. Yang W, Zhu D, Gan S, Dong X, Su J, Li W, et al. Dorzagliatin add-on therapy to metformin in patients with type 2 diabetes: a randomized, double-blind, placebo-controlled phase 3 trial. *Nat Med*. 2022;28(5):974–81.
17. Pfefferkorn JA, Guzman-Perez A, Oates PJ, Litchfield J, Aspnes G, Basak A, et al. Designing glucokinase activators with reduced hypoglycemia risk: discovery of N, N-dimethyl-5-(2-methyl-6-(5-methylpyrazin-2-yl)-carbamoyl)benzofuran-4-yloxy)pyrimidine-2-carboxamide as a clinical candidate for the treatment of type 2 diabetes mellitus. *Medchemcomm*. 2011;2(9):828–39.
18. Amin NB, Aggarwal N, Pall D, Paragh G, Denney WS, Le V, et al. Two dose-ranging studies with PF-04937319, a systemic partial activator of glucokinase, as add-on therapy to metformin in adults with type 2 diabetes. *Diabetes Obes Metab*. 2015;17(8):751–9.
19. Denney WS, Denham DS, Riggs MR, Amin NB. Glycemic effect and safety of a systemic, partial glucokinase activator, PF-04937319, in patients with type 2 diabetes mellitus inadequately controlled on metformin: a randomized, crossover, active-controlled study. *Clin Pharmacol Drug Dev*. 2016;5(6):517–27.
20. Liu D, Du Y, Yao X, Wei Y, Zhu J, Cui C, et al. Safety, tolerability, pharmacokinetics, and pharmacodynamics of the glucokinase activator PB-201 and its effects on the glucose excursion profile in drug-naïve Chinese patients with type 2 diabetes: a randomised controlled, crossover, single-centre phase 1 trial. *EClinicalMedicine*. 2021;42: 101185.
21. Bergstrand M, Karlsson MO. Handling data below the limit of quantification in mixed effect models. *AAPS J*. 2009;11(2):371–80.
22. Gao W, Jusko WJ. Modeling disease progression and rosiglitazone intervention in type 2 diabetic Goto-Kakizaki rats. *J Pharmacol Exp Ther*. 2012;341(3):617–25.
23. Borzilleri KA, Pfefferkorn JA, Guzman-Perez A, Liu SP, Qiu XY, Chrunyk BA, et al. Optimizing glucokinase activator binding kinetics to lower in vivo hypoglycemia risk. *Medchemcomm*. 2014;5(6):802–7.
24. Borg R, Kuenen JC, Carstensen B, Zheng H, Nathan DM, Heine RJ, et al. Associations between features of glucose exposure and A1C: the A1C-Derived Average Glucose (ADAG) study. *Diabetes*. 2010;59(7):1585–90.
25. Gaitonde P, Garhyan P, Link C, Chien JY, Trame MN, Schmidt S. A comprehensive review of novel drug-disease models in diabetes drug development. *Clin Pharmacokinet*. 2016;55(7):769–88.
26. Savic RM, Karlsson MO. Importance of shrinkage in empirical bayes estimates for diagnostics: problems and solutions. *AAPS J*. 2009;11(3):558–69.
27. Sharma R, Litchfield J, Atkinson K, Eng H, Amin NB, Denney WS, et al. Metabolites in safety testing assessment in early clinical development: a case study with a glucokinase activator. *Drug Metab Dispos*. 2014;42(11):1926–39.

Springer Nature or its licensor (e.g. a society or other partner) holds exclusive rights to this article under a publishing agreement with the author(s) or other rightsholder(s); author self-archiving of the accepted manuscript version of this article is solely governed by the terms of such publishing agreement and applicable law.

Authors and Affiliations

Ling Song^{1,2,3} · Fangrui Cao¹ · Shu Niu¹ · Michael Xu⁴ · Ruifang Liang⁴ · Ke Ding⁴ · Zhigang Lin⁴ · Xueting Yao¹ · Dongyang Liu^{1,3,5} 

✉ Xueting Yao
liangmuxueting@sina.com

✉ Dongyang Liu
liudongyang@vip.sina.com

¹ Drug Clinical Trial Center, Peking University Third Hospital, Beijing 100191, China

² Department of Obstetrics and Gynecology, Peking University Third Hospital, Beijing, China

³ Institute of Medical Innovation and Research, Peking University Third Hospital, Beijing 100191, China

⁴ PegBio Co., Ltd., Suzhou, Jiangsu, China

⁵ Beijing Key Laboratory of Cardiovascular Receptors Research, Peking University Third Hospital, Beijing, China